Running title: Characterization of Arabidopsis CMP-KDO synthetase

Corresponding author: Masaru Kobayashi

Laboratory of Plant Nutrition, Division of Applied Life Sciences,

Graduate School of Agriculture, Kyoto University,

Kyoto 606-8502, Japan.

Tel: +81-75-753-6407

Fax: +81-75-753-6107

E-mail: kobayashi.masaru.8e@kyoto-u.ac.jp

Subject areas

Proteins, Enzymes and Metabolism

Growth and Development

Number of black and white figures: 0

Number of black and white tables: 2

Number of color figures: 5

Number of color tables: 0

Characterization of Arabidopsis CTP:3-deoxy-D-*manno*-2-octulosonate cytidylyltransferase (CMP-KDO synthetase), the enzyme that activates KDO during rhamnogalacturonan II biosynthesis

Masaru Kobayashi[1], Nagisa Kouzu[1], Akina Inami[1], Kiminori Toyooka[2], Yuki Konishi[1], Ken Matsuoka[3], Toru Matoh[1]

[1] Division of Applied Life Sciences, Graduate School of Agriculture, Kyoto University, Kyoto 606-8502, Japan

[2] RIKEN Plant Science Center, Tsurumi-ku, Yokohama 230-0045, Japan

[3] Faculty of Agriculture, Kyushu University, Higashi-ku, Fukuoka 812-8581, Japan

Abbreviations:

B, boron; BSA, bovine serum albumin; CKS, CMP-KDO synthetase; DAPI, 4',6-diamidino-2-phenylindole; GFP, green fluorescent protein; IPTG, isopropyl-β-D-thiogalactoside; KDO, 3-deoxy-D-*manno*-2-octulosonic acid; KDOS, KDO-8-phosphate synthase; mRFP, monomeric red fluorescent protein; PH, prolyl hydroxylase; RG-II, rhamnogalacturonan II; TBS, Tris-buffered saline.

Abstract

In plant cells, boron (B) occurs predominantly as a borate ester associated with the rhamnogalacturonan II (RG-II) complex, but the function of this B-RG-II complex has yet to be investigated. 3-Deoxy-D-*manno*-2-octulosonic acid (KDO) is a specific component monosaccharide of RG-II. Mutant plants defective in KDO biosynthesis are expected to have altered RG-II structure, and would be useful for studying the physiological function of the B-RG-II complex. Here, we characterized Arabidopsis CTP:KDO cytidylyltransferase (CMP-KDO synthetase; CKS), the enzyme activating KDO as a nucleotide sugar prior to its incorporation into RG-II. Our analyses localized the Arabidopsis CKS protein to mitochondria. The Arabidopsis *CKS* gene occurs as a single-copy gene in the genome, and we could not obtain *cks* null mutants from the T-DNA insertion lines. Analysis using +/*cks* heterozygotes in the *quartet1* background demonstrated that the *cks* mutation rendered pollen infertile through the inhibition of pollen tube elongation. These results suggest that KDO is an indispensable component of RG-II, and that the complete B-RG-II complex is essential for the cell wall integrity of rapidly growing tissues.

Keywords

Arabidopsis, boron, CMP-KDO synthetase, KDO, pectin, rhamnogalacturonan II

Introduction

Boron (B) is an essential micronutrient for vascular plants, and its deficiency causes various metabolic disorders and cell death (Koshiba et al. 2009, 2010). Plants take up B as boric acid from the soil. Boric acid forms esters with compounds that have two hydroxyl groups in a *cis*-configuration. To date, several borate esters have been identified in plants. The apiosyl residue in pectic polysaccharides forms borate esters that are sufficiently stable under physiological conditions. The apiosyl residue occurs in apiogalacturonan of *Lemna* (Hart and Kindel 1970) and rhamnogalacturonan II (RG-II) of every plant species (Matoh et al. 1996). In several plant species, B can be translocated as a complex with sorbitol or mannitol (Brown and Shelp 1997). Some membrane-associated proteins are also proposed to form complexes with B (Wimmer et al. 2009), but their stability and physiological relevance remain elusive.

RG-II is a structurally complex pectic polysaccharide present in the primary cell wall. RG-II consists of a linear 1,4-linked α-D-galacturonic acid backbone with four distinct side chains, two of which contain apiosyl residues. Boric acid forms a diester with two apiosyl residues from separate RG-II molecules, thereby covalently cross-linking two RG-II molecules as a dimer. In suspension cultured tobacco cells, essentially all the cellular B is localized in the cell wall (Matoh et al. 1992), and nearly 80% of the cell wall B is found in the form of this B-RG-II complex (Kobayashi et al. 1997). The predominant occurrence of B as the B-RG-II complex suggests that this complex represents the primary, if not the only, form of B functional in plant cells. RG-II is released from cell walls through the action of endo-polygalacturonase. Therefore, it is likely that in the cell wall, the RG-II is connected to a stretch of linear 1,4-linked α-D-galacturonic acids, and together they form regions of pectic macromolecules. Hence, the B-RG-II linkage is considered to cross-link the macromolecule to form a supramolecular pectic network. Consistent with this idea, we previously showed that most of the pectic polysaccharides in radish root cell walls remain insoluble unless the B-RG-II complex is broken (Kobayashi et al. 1999). The pectic network thus formed is critical for building the structure of

the cell wall. When tobacco BY-2 cells are maintained under a limited supply of B, more than 60% of the RG-II in their cell wall remains unconjugated with B, and their cell walls are swollen (Matoh et al. 2000). In addition, Fleischer et al. (1998) showed that cell wall porosity, which is probably determined by the density of cross-linking in pectic polysaccharides, increases under B-deficient conditions in suspension-cultured *Chenopodium album* cells.

Although the findings mentioned above demonstrate the significance of the B-RG-II complex in cell wall architecture, the precise function and the character of this complex in vivo have yet to be investigated. Mutant plants defective in RG-II structure could be useful for such a study. Arabidopsis *mur1* is a mutant of GDP-D-mannose-4,6-dehydratase, which is involved in the synthesis of GDP-L-fucose (O'Neill et al. 2001). The tobacco (*Nicotiana plumbaginifolia*) mutant *nolac-H18* is a mutant of a glucuronosyltransferase (Iwai et al. 2002). RG-IIs in these mutants are structurally altered to lack L-fucosyl (*mur1*) or D-glucuronosyl (*nolac-H18*) residues in their side chains, and the B-RG-II linkages are less stable than that of the wild-type. The mutant plants show inhibited leaf expansion, intercellular attachment, or reproductive growth. These results suggest that the B-RG-II linkage is essential for normal plant growth and development. However, since the occurrence of L-fucose and D-glucuronic acid are not exclusive to RG-II, it remains uncertain whether or not the observed phenotypes are due solely to defects in B-RG-II linkages. To address this ambiguity, it is necessary to characterize mutants lacking RG-II-specific monosaccharides.

The eight-carbon sugar acid 3-deoxy-D-*manno*-2-octulosonic acid (KDO) is one of the component monosaccharides of RG-II. KDO also occurs in bacterial lipopolysaccharides as the linker between lipid A and extracellular core oligosaccharides (Raetz 1990). During the course of this study, Li et al. (2011) reported that plants may also synthesize a lipid A-like molecule. However, it remains to be demonstrated whether or not KDO is indeed attached to the putative lipid A-like molecule as is the case for bacterial lipid A, and so far RG-II is the only molecule that has been proven to contain KDO in plants. Hence, the RG-II KDO residue is a good

candidate as a target for modifying the structure of the B-RG-II complex. In bacteria, KDO is first produced as KDO-8-phosphate through the action of KDO-8-phosphate synthase (KDOS), which catalyzes the aldol condensation of D-arabinose-5-phosphate and phosphoenolpyruvate. The KDO-8-phosphate is dephosphorylated to KDO, and the resulting KDO is then activated as CMP-KDO by CTP:KDO cytidylyltransferase (CMP-KDO synthetase, CKS; EC 2.7.7.38) to serve as the substrate for KDO transferase. A similar pathway is thought to exist in plants, because plant genomes contain sequences homologous to the bacterial enzymes. Indeed, KDOS and CKS have been cloned from plants (Matsuura et al. 2003, Royo et al. 2000). Inhibition at any step of this pathway is expected to reduce or block the incorporation of KDO into RG-II. Here, we focus on Arabidopsis CKS as the target, since the putative CKS appears not to be redundant in the genome. A plant CKS was first cloned from maize by Royo et al. (2000) as the gene encoding a protein with a similar amino acid sequence and activity to the bacterial CKS. Recently, Misaki et al. (2009) reported the enzymatic characterization of the putative Arabidopsis CKS. However, to our knowledge, there is no report on the effects of a CKS mutation in plants. To gain further insight into the in vivo function of the B-RG-II complex and the specific contribution of KDO residues to its function, we characterized the putative Arabidopsis CKS in detail and analyzed its T-DNA insertion mutants. Our data demonstrate that the *cks* mutation impairs pollen function, suggesting that the B-RG-II complex plays a particularly important role in reproductive growth, possibly through maintaining the cell wall integrity of rapidly growing tissues such as pollen tubes.

Results

At1g53000 Encodes Arabidopsis CKS

Royo et al. (2000) cloned maize *CKS* (*ZmCKS*) as the gene homologous to the bacterial *CKS*. Other sequences with strong similarities to these sequences exist in various plant species, and are available in public databases (Fig. 1). The sequence in Arabidopsis (*At1g53000*) appears

to exist as a single-copy gene in the genome. As has been reported for the maize CKS protein, the deduced amino acid sequence of this putative Arabidopsis *CKS* has a N-terminal transit peptide-like sequence, which is absent from the bacterial CKS (Fig. 1). To confirm that the gene represents Arabidopsis CKS, we prepared a recombinant protein of this gene and compared its enzymatic properties with those of known CKS proteins. When the coding sequence excluding the putative transit peptide was expressed in *Escherichia coli*, the lysate exhibited higher CMP-KDO synthesis activity than that of the uninduced control (Fig. 2a, b). The recombinant protein was partially purified using the attached hexahistidine tag and its enzymatic properties were further characterized. When analyzed using CTP as the nucleotide donor, the recombinant enzyme showed the highest activity at pH 9.5 (Fig. 2c). When assayed at pH 9.5, CTP was the most favorable nucleotide donor (Fig. 2d). These characteristics are essentially the same as those reported for maize CKS (Royo et al. 2000), supporting that the gene represents Arabidopsis CKS. Hereafter we refer to this gene as *AtCKS*.

Subcellular localization of AtCKS

To investigate the subcellular localization of AtCKS protein, green fluorescent protein (GFP) was fused to the C-terminus of full-length AtCKS, and the construct was expressed in tobacco BY-2 cells under the control of the cauliflower mosaic virus 35S RNA promoter. The GFP signal exhibited a punctate pattern (Fig. 3a). When the transformed cells were fed with MitoTracker dye that specifically stains mitochondria, the MitoTracker signal colocalized with GFP fluorescence (Fig. 3a). The colocalized GFP and MitoTracker signal was also observed in roots of Arabidopsis expressing the same AtCKS:GFP fusion protein (data not shown). We also examined possible localization of AtCKS:GFP in Golgi apparatus. However, the fluorescence signals from AtCKS:GFP did not colocalize with those from monomeric red fluorescent protein (mRFP) fused to prolyl hydroxylase (PH), which is predominantly localized in *cis*-Golgi (Yuasa et al. 2005) (Fig. 3b). The result suggests that the AtCKS:GFP is not associated with Golgi

apparatus. This assumption was further supported by an observation that the distribution of GFP fluorescence was not affected by brefeldin A, an inhibitor of anterograde vesicle transport from the endoplasmic reticulum to Golgi apparatus (Supplementary Fig. S1). Signals from mitochondria were also observed with immunogold labeling using anti-CKS antisera. On sections of Arabidopsis root tip prepared by a high pressure freezing and freeze-substitution method (Toyooka et al. 2009), we found the signals on mitochondria, particularly around the outer or inner membranes (Fig. 3c). Together, these results suggest that CKS is targeted to mitochondria in plant cells. A fusion protein in which GFP was fused to the first 55 amino acids of AtCKS showed the same punctate pattern as the full length AtCKS:GFP fusion protein (data not shown), indicating that the N-terminal region of AtCKS is sufficient to target the protein to mitochondria.

To analyze further the subcellular localization of CKS, a mitochondria-enriched fraction was prepared, treated with thermolysin, and analyzed by immunoblotting. CKS was mostly resistant to thermolysin in the absence of detergent (Fig. 3d), whereas it was digested almost completely when the mitochondrial membrane was permeabilized with Triton X-100. This detergent-dependent proteolysis was similar to that observed with alternative oxidase (Elthon et al. 1989), which is associated with the inner membrane of the mitochondrion (Fig. 3d). This result suggests that the epitopes for the CKS antiserum were protected by the membrane. The CKS antiserum used here was raised against a recombinant AtCKS protein lacking the N-terminal leader sequence. Thus, it is suggested that CKS, or its catalytic domain at least, is localized inside the mitochondrion.

cks Insertion mutants are impaired in male gametophytic transmission

To evaluate the physiological significance of CKS, we attempted to isolate a CKS loss-of-function mutant of Arabidopsis from T-DNA insertion lines. We obtained seeds of three independent T-DNA insertion lines (SALK_008109, SALK_021302, SALK_052743; Fig. 4a)

from the Arabidopsis Biological Resource Center (ABRC), but identified no homozygous (*cks*/*cks*) mutants in these lines (Fig. 4b, Table 1). We also obtained seeds of SALK_008109 and SALK_052743 from the Salk HM Collection (a collection of homozygous T-DNA mutant lines) but genomic PCR analyses revealed that these seeds were heterozygous (data not shown). Thus, we consider that a *cks* null mutant cannot be obtained. The heterozygous (+/*cks*) plants were indistinguishable from wild-type (+/+) plants when grown at 24°C under continuous light. The abundance of *AtCKS* transcripts was similar in +/*cks* and +/+ plants (Fig. 4c).

The selfed progeny from +/*cks* plants segregated 1:1 for +/+ and +/*cks* plants (Table 1), suggesting that the *cks* mutation affected gametophytic performance. Genetic complementation tests were performed by transforming +/*cks* plants (SALK_052743) with a 4.1-kb genomic fragment which contained the 0.7-kb region upstream of the initiation codon and the entire *CKS* coding sequence (Fig. 4a). A T_2 plant that was +/*cks* but homozygous for the *CKS* transgene was selected and allowed to self-pollinate. The progenies segregated 19:25:15 for +/+:+/*cks*:*cks*/*cks* plants. The occurrence of *cks*/*cks* plants showed that the *CKS* transgene complemented the T-DNA mutant phenotype, confirming that the T-DNA insertion in the *CKS* locus caused the genetic distortion.

We then analyzed genetic transmission of the *cks* allele through the male and female by performing cross-pollination. Table 2 shows representative results of three independent experiments. There was no transmission of the mutant allele through the male, while transmission through the female appeared to be normal. This result demonstrates that the *cks* mutation specifically affected male gametophyte development and/or functions.

cks Mutation impairs pollen tube elongation

To address the role of CKS in pollen development and functionality, we crossed *quartet1* (*qrt1*) mutant plants (Preuss et al. 1994) with +/*cks* plants. Pollen grains of F_2 plants with the +/*cks*; *qrt1*/*qrt1* genotype were subjected to 4',6-diamidino-2-phenylindole (DAPI) and

Alexander staining. In *qrt1* mutant plants, the four pollen grains derived from one single microspore mother cell do not separate even after maturation (Preuss et al. 1994). Thus, a tetrad of four pollen grains from +/*cks*; *qrt1*/*qrt1* mutants contains two + and two *cks* mutant grains. If the *cks* mutation causes developmental defects in pollen, two pollen grains in a tetrad would show abnormalities. However, the four pollen grains in a tetrad from +/*cks* plants were indistinguishable morphologically. All grains in the tetrad were viable according to Alexander staining (Fig. 5a), and showed normal DAPI staining patterns, that is, one vegetative nucleus with diffuse fluorescence and two smaller degenerative nuclei with more condensed fluorescence (Fig. 5b). This result suggests that pollen development was not affected by the *cks* mutation.

We then carried out an in vitro germination test of mutant pollen. Since the germination rates of both +/+ and +/*cks* pollen were rather low, it was difficult to judge whether or not the germination rate was decreased by the mutation. However, we frequently observed +/*cks*; *qrt1*/*qrt1* tetrads with three pollen tubes (Fig. 5c). This observation indicates that at least one of the *cks* pollen grains in the tetrad germinated, and therefore germination is not blocked by the mutation. Among the pollen tubes germinated from +/*cks*; *qrt1*/*qrt1* tetrads, we often observed short and fat pollen tubes, which were seldom found within the +/+; *qrt1*/*qrt1* tetrads (Fig. 5c). When the frequency distribution of pollen tube lengths was plotted, +/*cks*; *qrt1*/*qrt1* tetrads showed a peak at 0–100 nm, whereas +/+; *qrt1*/*qrt1* tetrads showed a peak at 200–300 nm (Fig. 5d). These results suggest that the *cks* mutation impairs pollen tube elongation.

Discussion

Arabidopsis genome contains a single-copy gene which encodes a protein highly homologous to maize CKS (ZmCKS; Royo et al. 2000). We demonstrated that the recombinant protein of this putative Arabidopsis *CKS* showed almost the same enzymatic properties as those reported for ZmCKS (Royo et al. 2000). This result confirms that the gene indeed represents the

Arabidopsis *CKS*. During the course of this study, Misaki et al. (2009) published an enzymatic characterization of a recombinant protein of the same *AtCKS* gene. The recombinant AtCKS they prepared showed distinct enzymatic properties to those observed in this study and reported for ZmCKS: the recombinant AtCKS they prepared did not utilize UTP, whereas UTP could partially replace CTP for the AtCKS described in the present study (Fig. 2d). In addition, their recombinant enzyme exhibited the highest activity at pH 8.0, which is lower than that observed in this study (pH 9.5, Fig. 2c). These differences may be due to the difference in the region of the protein expressed. Misaki et al. (2009) expressed the full length AtCKS sequence, whereas we expressed a partial sequence without the N-terminal putative sorting signal sequence. The N-terminal leader sequence was shown to function as a mitochondrial targeting signal in this study, but it may also affect the catalytic properties of this enzyme.

Misaki et al. (2009) reported that *AtCKS* gene was ubiquitously expressed in the leaves, stems, roots, and siliques of Arabidopsis. In this study, we found that the *cks* mutation impaired pollen function. Expression of *CKS* in mature pollen and growing pollen tubes was confirmed by the analysis of publicly available microarray data using Arabidopsis eFP browser (Winter et al. 2007; http://bar.utoronto.ca/efp/cgi-bin/efpWeb.cgi). The analysis also suggests that the *CKS* gene expression is particularly high in shoot apex, seedling root, developing and dry seeds, stigma and ovules. Preferential expression in meristematic tissues is similar to the case for the gene encoding an isoform of KDOS (KdsA2; At1g16340) (Delmas et al. 2009), which is upstream to CKS in KDO biosynthesis pathway. In fact, global coexpression analyses using Expression Angler (Toufighi et al. 2005; http://bar.utoronto.ca/ntools/cgi-bin/ntools_expression_angler.cgi) or ATTED-II (Obayashi et al. 2009; http://atted.jp) programs indicate that the expression of *AtCKS* and *AtKdsA2* are highly correlated, suggesting that the enzymes for KDO biosynthesis pathway are transcriptionally co-regulated.

Analyses using AtCKS-GFP fusion protein or anti-CKS antibody suggest that the AtCKS protein is localized in mitochondria (Fig. 3a-c). These observations are consistent with a report that this protein is present in the mitochondrial proteome (Heazlewood et al. 2004), and provide, to our knowledge, the first direct evidence of the occurrence of nucleotide sugar-synthesizing enzyme in mitochondria. The observed resistance to proteolysis in the absence of detergent (Fig. 3d) suggests that the CKS is inside the outer membrane of the mitochondrion. At present the physiological reasons for such compartmentalization remain unclear, since the transfer of KDO from CMP-KDO to nascent RG-II probably occurs in the Golgi apparatus, where the pectic polysaccharides are synthesized (Mohnen 2008). Phylogenetic analysis suggests that the plant *CKS* gene was originally acquired from endosymbiotic or endoparasitic eubacteria through a horizontal gene transfer (Royo et al. 2000). Subsequently, a transit peptide would have been added to its N-terminus to send the protein to mitochondria. Thus it is suggested that the CKS protein has some physiological roles in this organelle. Recently, Li et al. (2011) have reported that plants may have a bacterial lipid A-like molecule. Lipid A is an acylated disaccharide of glucosamine to which KDO-(2,4)-KDO disaccharide is attached to build cell surface lipopolysaccharides. Arabidopsis genome encodes orthologs of bacterial enzymes for the lipid A biosynthesis, including LpxA, LpxB, LpxC, LpxD and LpxK, and the mutant plants for these genes accumulate lipid A precursors identified in *E. coli*. In addition, Arabidopsis has an ortholog of bacterial KDO transferase (KdtA), which transfers KDO to lipid A from CMP-KDO (Séveno et al. 2010). The Arabidopsis Lpx and KdtA proteins are localized in mitochondria (Séveno et al. 2010, Li et al. 2011). Although so far it has not been demonstrated that KDO is indeed attached to the plant lipid A-like molecule, these results collectively imply that plant mitochondria synthesize KDO_2-lipid A-like molecule, as their eubacterial ancestor did. If this is the case, it is conceivable that the activation of KDO for synthesizing the putative KDO_2-lipid A molecule occurs in mitochondria, and plants may employ the system for synthesizing the RG-II KDO residues as well. Takashima et al. (2009) identified putative nucleotide sugar transporters

in Arabidopsis and rice, which are capable of transporting CMP-sialic acid into the Golgi lumen. Since the presence of sialic acid in plants has not been established yet, the authors speculated that the physiological substrate of these proteins is CMP-KDO. The occurrence of transporters importing CMP-KDO into the Golgi lumen supports our speculation that CMP-KDO is synthesized outside the Golgi apparatus, where the sugar nucleotide is utilized to make RG-II.

The possible existence in plants of KDO-containing molecule(s) other than RG-II raises a question as to whether the phenotypes of *cks* mutant plants can be ascribed to a defective RG-II structure. However, since null mutants for *Lpx* genes or *KdtA* are viable and show no obvious phenotype compared to wild type plants (Séveno et al. 2010, Li et al. 2011), the putative KDO_2-lipid A-like molecule, if any, appears to be dispensable under normal growth conditions. Thus we assume that the impaired function of *cks* mutant pollens is due, at least to a major degree, to the inhibition of KDO incorporation into RG-II.

We could not obtain *cks* knockout mutant plants. This was because *cks* mutant pollen was infertile, as shown by the reciprocal test crosses (Table 2). The *cks* mutation did not block pollen maturation and germination, but impaired pollen tube elongation (Fig. 5). Recently, Delmas et al. (2008) reported that the mutation of *KDOS* caused male sterility via inhibiting pollen tube elongation. The observation is consistent with our results, and confirms the importance of RG-II KDO residues in pollen function. Short and fat pollen tubes were observed frequently among the in vitro germinated pollen grains of +/*cks* plants. Since pollen grains of +/+ plants did not show these characteristics, this morphology appears to be associated with the *cks* mutation. In *cks* mutant pollen, activation and hence incorporation of KDO into RG-II is expected to be inhibited. The resulting structurally defective RG-II, if produced, may not form a stable complex with borate, as has been shown with the other RG-II mutants (Iwai et al. 2002, O'Neill et al. 2001). This may lead to weakened cell wall structure, since the B-RG-II complex significantly contributes to the tensile strength of the cell wall (Ryden et al. 2003). Pollen tubes with such a weakened cell wall may swell radially, but not elongate efficiently. Significantly,

transmission of the *cks* mutant allele through the female was not impaired (Table 2). In addition, the *cks* mutation apparently did not block pollen formation and development (Fig. 5a, b). Thus we consider that the haploid gametophytes with the defective RG-II can still maintain their cell wall structure, although they may divide and grow rather slowly, but the intact B-RG-II complex is indispensable for rapidly growing tissues such as pollen tubes. This is consistent with the fact that cell elongation is more sensitive to B deficiency than cell division (Fleischer et al. 1998). It is also known that the plant requirement for B is particularly high at the reproductive stage, and B-deficient plants may fail to set seeds even if they show no sign of deficiency during their vegetative growth period. Our data suggest that the formation of the B-RG-II complex is critical for pollen performance and fertilization. Failure to form the B-RG-II complex may be the cause of reduced seed setting under B deficiency.

Because of the difficulty in obtaining sufficient RG-II from pollen, we have not yet determined the effect of the *cks* mutation on RG-II molecular structure. RNAi plants with decreased *CKS* expression in their vegetative tissues are now being characterized in our laboratory, and the analysis of their cell wall will answer this question. The absence or decrease of the CKS protein should inhibit the incorporation of KDO into the RG-II side chain. Since the KDO residue links the side chain and backbone in RG-II, displacement of this residue makes construction of the entire KDO-containing side chain impossible. Thus *cks* mutation may lead to the formation of mutant RG-II lacking a KDO-containing side chain. The change may also suppress the assembly of the RG-II domain itself. Since polysaccharides are synthesized without a template, their assembly depends on the substrate specificity of glycosyltransferases that strictly recognize the acceptor structure. Thus, the disappearance of one side chain may also affect the formation of other side chains. At the same time, however, we cannot exclude the possibility that the mutant gametophytes still contain the intact RG-II with KDO residues, although in a smaller amount. RG-II contains another 2-keto-3-deoxysugar, 3-deoxy-D-*lyxo*-2-heptulosaric acid (DHA), which is structurally similar to KDO (Stevenson et

al. 1988). If the biosynthesis and incorporation of DHA into the RG-II side chain occur in a similar way to those of KDO, plants may have some nucleotidyl transferase acting on DHA. Such enzymes may substitute in part for CKS. Further analysis of the polysaccharides in *cks* mutants will give us valuable information on the biosynthesis of pectic polysaccharides.

Materials and Methods

Plant materials

Arabidopsis (*Arabidopsis thaliana*) plants were grown under continuous light at 24°C. Ecotype Columbia-0 was used as the wild-type unless otherwise stated. Arabidopsis T-87 cells were obtained from the RIKEN Bioresource Center and maintained as described (Axelos et al. 1992). Tobacco BY-2 cells (*Nicotiana tabacum* cv. Bright Yellow-2) were maintained as described (Nagata et al. 1981).

Genotyping of plants

Seeds of T-DNA insertion lines (SALK_008109, 008109C, 021302, 052743, and 052743C) and *qrt1-2* mutant plants were obtained from ABRC. Primers for the identification of insertion lines were designed using the SALK T-DNA verification primer design program (http://signal.salk.edu/tdnaprimers.2.html) as follows: 1L, 5'-ttgggagaggtcgaagttagc-3' and 1R, 5'-tccaagatgaagcatgtacgg-3' for SALK_052743 and SALK_052743C; 2L, 5'-aatgtgtcaaaaatcctagccg-3' and 2R, 5'-ttttatcctcagagctttgattcg-3' for SALK_008109 and SALK_008109C; 3L, 5'-caatcactctgagccatttttaac-3' and 3R, 5'-tgcttcatcttggaattcagg-3' for SALK_021302; and LBa1, 5'-tggttcacgtagtgggccatcg-3' for the T-DNA left border (Fig. 4a). Small pieces of leaves were taken from individual plants and crushed with a micropipette tip in 20 µl 200 mM Tris-HCl, 250 mM NaCl, 25 mM EDTA, and 0.5% (w/v) SDS, pH 8.0. Then, 20 µl 2-propanol was added to each tube and the mixture was centrifuged at 12,000×*g* for 5 min.

The supernatant was discarded, and the precipitate including leaf debris was resuspended in 20 µl 10 mM Tris-HCl, 1 mM EDTA, pH 8.0. An aliquot of the suspension was used as the template for PCR using GoTaq DNA polymerase (Promega, Madison, WI, USA).

CKS transcript abundance in +/+ and +/*cks* (SALK_52743) plants was compared with RT-PCR. Total RNA was extracted from leaves of either +/+ or +/*cks* plants using an RNeasy Plant Mini kit (Qiagen) according to the manufacturer's instructions. First strand cDNA was synthesized using the $d(T)_{18}$ primer and ReverTraAce reverse-transcriptase (TOYOBO, Osaka, Japan), and subjected to semiquantitative RT-PCR with the primers S, 5'-gtgttgtcgtggatttggtg-3' and A, 5'-taaggaatcaaaccccttgag-3' (Fig. 4a). *Actin* was amplified to calibrate the amounts of cDNA using the primers 5'-gtggtcgtacaaccggtattg-3' and 5'-gggctggaacaagacttctg-3'.

Analysis of gametophytes

Cross-pollination was carried out as described by Johnson-Brousseau and McCormick (2007). To examine transmission of the *cks* genotype, ecotype Landsberg *erecta* (L*er*) was used as the wild-type parent, and each progeny was confirmed to be a hybrid of L*er* and Col (SALK T-DNA lines) based on the simple sequence length polymorphism at PAT1.2 (TAIR Accession No. Genetic Marker: 1945631).

In vitro germination was carried out as described (Boavida and McCormick 2007), on a medium containing 1.6 mM $B(OH)_3$, 5 mM $CaCl_2$, 5 mM KCl, 1 mM $MgSO_4$, 0.35 M sucrose, pH 7.5, and 1.5% (w/v) low melting-point agarose (Wako Pure Chemicals, Osaka, Japan). Pollen grains were allowed to germinate,and then elongation of the pollen tubes was examined under a microscope after overnight incubation. The lengths of elongated tubes were measured using ImageJ software (http://rsbweb.nih.gov/ij/).

The viability of mature pollen grains was inspected by Alexander staining (Alexander 1969). To observe pollen DNA, pollen grains were stained with 1 $mg \cdot liter^{-1}$ DAPI, 0.1% (w/v) Tween 20

in 10 mM Tris-HCl, pH 8.0, and then examined under a fluorescent microscope (BX51, Olympus, Tokyo, Japan).

Genetic complementation

BAC clone F8L10 was obtained from ABRC, and a 4.1-kb fragment containing the AtCKS coding sequence and its upstream sequence was cut from the plasmid with *Sac*I and *Bam*HI. The fragment was cloned into the *Sac*I/*Bam*HI site of pCAMBIA 1302 (http://www.cambia.org), and the resulting plasmid was introduced into *Agrobacterium tumefaciens* C58C1Rif^{R}. The +/*cks* mutant plants (SALK_52743) were transformed with this construct by the floral dip method (Clough and Bent 1998). An individual heterozygous for the T-DNA insertion (+/*cks*) and homozygous for the *CKS* transgene was selected from the T_2 generation and allowed to self-pollinate. The progenies were analyzed for segregation of the *cks* allele by genomic PCR. The presence of the T-DNA insertion was examined using a primer pair for the *nptII* gene; 5'-ggctattcggctatgactgg-3' and 5'-gcgataccgtaaagcacgag-3'. The endogenous *CKS* allele was detected using an upstream primer U, 5'-tttagcacagcggtgacatc-3', and a downstream primer D, 5'-accaaacaaagatcggttcg-3' (Fig. 4a). The *CKS* transgene does not include the annealing site for D, hence the intact endogenous *CKS* allele was selectively amplified with this set of primers. The PCR amplification was performed with KOD FX DNA polymerase (TOYOBO).

Subcellular localization analysis

AtCKS ORF was amplified by PCR from an Arabidopsis cDNA library, using a *Sal*I-linked forward primer 5'-ctcaccggagtcgacaaagtgatgtcg-3' and a *Nco*I-linked reverse primer 5'-gtggccatggacatgtttctttcgc-3'. The amplified product was digested with *Sal*I and *Nco*I, and first cloned into the *Sal*I/*Nco*I site of the vector CaMV35S-sGFP(S65T)-NOS3' (Chiu et al. 1996). Then, a 2.1-kb *Bam*HI-*Pst*I fragment containing the cauliflower mosaic virus 35S RNA

promoter and AtCKS:GFP cDNA was cut from the construct, and cloned into the *Bam*HI/*Pst*I site of the binary vector pCAMBIA 1380 (http://www.cambia.org). The resulting plasmid was introduced into *A. tumefaciens* EHA105. Transformation of tobacco BY-2 cells was carried out as described (An 1985). Transformed cells were selected on a hygromycin-containing plate and transferred to liquid medium. After several rounds of subculturing, cells were stained with 0.5 μM MitoTracker Red CMXRos (Cambrex Bio Science Walkersville, Walkersville, MD, USA) for 5 min, and examined for GFP and MitoTracker fluorescence using a confocal laser scanning microscope (FluoView FV500, Olympus).

For transient expression of AtCKS:GFP in cells expressing PH:mRFP, *Agrobacterium* harboring the binary vector was co-cultured with tobacco cells expressing PH:mRFP at 26ºC for 2 days, washed with fresh medium and further incubated with medium containing 200 mg l^{-1} cefotaxime for a day. Thereafter fluorescence of cells was visualized using a confocal laser scanning microscope (Toyooka et al. 2009).

Arabidopsis T87 cells subcultured for 7 d were collected by centrifugation and washed once with 0.4 M mannitol, 20 mM MES-KOH, pH 5.8. The cells were incubated at room temperature for 2 h with gentle agitation in 0.4 M mannitol, 20 mM MES-KOH, pH 5.8, 20 mM KCl, 10 mM $CaCl_2$, 0.1% (w/v) bovine serum albumin (BSA) containing 1% (w/v) Cellulase Onozuka R-10 and 0.2% (w/v) Macerozyme R-10 (Yakult Honsha, Tokyo, Japan). Protoplasts were collected by centrifugation at 100×*g* for 1 min, and washed twice with 0.4 M mannitol, 10 mM potassium phosphate, pH 7.2, and resuspended in 0.4 M mannitol, 10 mM potassium phosphate, 1 mM EDTA, 0.1% (w/v) BSA, 1 mM dithiothreitol, and protease inhibitor cocktail (EDTA-free, Nacalai Tesque, Kyoto, Japan), pH 7.2. The protoplast suspension was homogenized with a glass homogenizer, and the homogenate was centrifuged at 1,000×*g* for 5 min. The supernatant was further centrifuged at 12,000×*g* for 10 min, and the resulting pellet was used as the mitochondria-enriched fraction. The pellet was resuspended in 0.4 M mannitol, 10 mM potassium phosphate, 5 mM $MgSO_4$, 10 mM KCl, and protease inhibitor cocktail

(EDTA-free), pH 7.2. Aliquots of the suspension were incubated for 20 min on ice with or without 1% (w/v) Triton X-100 and 0.05 mg ml^{-1} thermolysin (Nacalai Tesque). The protease inhibitor cocktail does not inhibit thermolysin. Digestion was terminated by adding 5 mM EDTA and 1 volume of 2 × SDS sample dye, and boiling for 5 min.

Expression and characterization of recombinant AtCKS protein in bacteria

The AtCKS sequence without the N-terminal 42 amino acid residues was expressed in *E. coli*. The corresponding cDNA fragment was amplified by PCR with *Bam*HI-linked forward and reverse primers (5'-cgggatccaagccgggtcgtcggaat-3' and 5'-cgggatccttcgatgtctcacacacaa-3', respectively) from an Arabidopsis cDNA library (kindly provided by Dr. Daisaku Ohta). The fragment was digested with *Bam*HI and inserted into the *Bam*HI site of pET-16b (Novagen, Madison, WI, USA). After verification of the sequence integrity, the construct was introduced into *E. coli* BL21(DE3). Protein expression was induced with 0.2 mM isopropyl-β-D-thiogalactoside (IPTG) at 16°C for 12 h. Bacterial cells were lysed with lysozyme (1 mg/ml) and Triton X-100 (0.2%, w/v), and the recombinant protein was partially purified by binding of its N-terminal hexahistidine tag to a HiTrap Chelating HP column (GE Healthcare, Piscataway, NJ, USA). In a typical experiment, recombinant CKS protein from 250 ml culture was recovered in 1.5 ml column effluent.

The enzyme assay was carried out essentially as described previously (Royo et al. 2000) with some modifications. Briefly, CKS activity was assayed at 30°C in a 250-µl reaction mixture containing 5 µl enzyme preparation, 200 mM Tris-acetate buffer, 10 mM $MgCl_2$, 1.6 mM KDO, 10 mM CTP, UTP, or ATP, and 10 U inorganic pyrophosphatase (from *E. coli*, Sigma-Aldrich, St. Louis, MO, USA), pH 9.5. To analyze the pH dependence of the enzyme activity, the assay was carried out in each of the following buffers (all 200 mM): potassium phosphate, pH 7.5; Tris-HCl, pH 8.0 or 9.0; and Tris-acetate, pH 9.5, using 10 mM CTP as the nucleotide donor. Reactions were initiated by adding enzyme preparation. At determined time

intervals, 50-µl aliquots were withdrawn, mixed with 100 µl ice-cold ethanol, and centrifuged at 12,000×*g* for 5 min at 4°C. CMP-KDO in the supernatant was determined colorimetrically (Ray and Benedict 1982).

Antibody production

The recombinant CKS protein was expressed in *E. coli* BL21(DE3) with 0.5 mM IPTG at 37°C for 6 h. Inclusion bodies containing the expressed protein were recovered from the lysate by centrifugation at 12,000×*g* for 5 min at 4°C, and washed three times by suspending the pellet using a sonicator in Tris-buffered saline (TBS; 20 mM Tris-HCl, 150 mM NaCl, pH 7.6) supplemented with 0.5% (w/v) Triton X-100. The washed inclusion bodies were solubilized in 8 M urea, and purified on a HiTrap Chelating HP (GE Healthcare) column in the presence of 8 M urea. The eluted CKS protein was used to raise a polyclonal antibody in rabbits.

Immunoblotting

Proteins were separated by SDS-PAGE and blotted onto a polyvinylidene fluoride membrane (Hybond-P, GE Healthcare). After blocking with defatted milk, the membrane was incubated with primary antibody and then with horseradish peroxidase-conjugated secondary antibodies (Nacalai Tesque). The antibodies were diluted with an immunoreaction enhancer solution (Can Get Signal, TOYOBO) at 1:10,000 (anti-CKS), 1:500 (anti-AOX), or 1:30,000 (secondary antibodies). Blots were washed with phosphate-buffered saline (8.1 mM Na_2HPO_4, 1.5 mM KH_2PO_4, 137 mM NaCl, and 2.7 mM KCl, pH 7.4) supplemented with 0.1% (w/v) Tween 20 after incubation with antibodies. Signals were detected with SuperSignal West Pico (Pierce Biotechnology, Rockford, MD, USA) on Hyperfilm ECL (GE Healthcare).

Immunocytochemistry

Five-day-old Arabidopsis root tips were placed on a flat specimen carrier (Leica, Solms, Germany) and frozen in a high-pressure freezer (EM-PACT; Leica). The frozen samples were fixed with anhydrous acetone containing 1% (w/v) glutaraldehyde for 3–4 days at –80°C. The tubes containing the frozen samples were warmed at 3°C h^{-1} to –20°C, at 1°C h^{-1} to 4°C, and kept for 2 h at 4°C using an automatic freeze-substitution system (EM-AFS; Leica). The samples were washed with anhydrous acetone, replaced by anhydrous methanol, and then embedded in LR white resin (Electron Microscopy Sciences, Hatfield, PA, USA). The ultra-thin sections on nickel grids (400 mesh) were blocked with 10% (w/v) BSA in TBS for 30 min at room temperature. The sections were stained with CKS antibody purified using the Melon Gel IgG Spin Purification Kit (Pierce Biotechnology) for 1 h at room temperature. After being washed with 0.1% (w/v) Triton X-100 in TBS, sections were indirectly labeled with 12 nm colloidal gold particles coupled to goat anti-rabbit IgG (Jackson ImmunoResearch Laboratories, West Grove, PA, USA) for 30 min. After being washed with TBS and distilled water, grids were stained with 4% (w/v) aqueous uranyl acetate for 10 min and examined with a transmission electron microscope (JEM-1011; JEOL, Tokyo, Japan) at 80 kV. Images were acquired using a Gatan DualView CCD camera and Gatan Digital Micrograph software (Gatan Inc., Pleasanton, CA).

Funding

The Ministry of Education, Culture, Sports, Science and Technology of Japan Grant-in-Aid for Scientific Research on Priority Areas (No. 18056011 and 20053011 to MK and TM); The Ministry of Education, Culture, Sports, Science and Technology of Japan Grant-in-Aid for Scientific Research on Innovative Areas (No. 23119509 to MK); Japan Society for Promotion of Science Grant-in-Aid for Scientific Research (C) (No. 20580062 to MK).

Acknowledgments

We are grateful to Mr. Hiroshi Tajima for his contribution to this study. We also thank Ms. Takako Kawai, Ms. Mayumi Wakazaki, and Ms. Yumi Goto (RIKEN Plant Science Center) for their assistance with electron microscopy, Dr. Kiyotaka Okada (National Institute for Basic Biology) for technical advice on in vitro pollen germination, Dr. Ikuo Nishida (Saitama University) for valuable discussion, Dr. Thomas Elthon (University of Nebraska-Lincoln) for the alternative oxidase antibody, Dr. Yasuo Niwa (Shimane University) for sGFP vectors, Dr. Daisaku Ohta (Osaka Prefectural University) for the Arabidopsis cDNA library, Dr. Tetsuro Okuno and Dr. Masanori Kaido (Kyoto University) for the use of the confocal laser scanning microscope, and the Salk Institute Genomic Analysis Laboratory for providing the Arabidopsis T-DNA insertion mutants.

References

Alexander, M.P. (1969) Differential staining of aborted and nonaborted pollen. *Stain Technol.* 44: 117–122.

An, G. (1985) High efficiency transformation of cultured tobacco cells. *Plant Physiol*. 79: 568-570.

Axelos, M., Curie, C., Mazzolini, L., Bardet, C. and Lescure, B. (1992) A protocol for transient gene expression in *Arabidopsis thaliana* protoplasts isolated from cell suspension cultures. *Plant Physiol. Biochem.* 30:123-128.

Boavida, L.C. and McCormick, S. (2007) Temperature as a determinant factor for increased and reproducible *in vitro* pollen germination in *Arabidopsis thaliana*. *Plant J*. 52: 570-582.

Brown, P.H. and Shelp, B.J. (1997) Boron mobility in plants. *Plant Soil* 193: 85-101.

Chiu, W., Niwa, Y., Zeng, W., Hirano, T., Kobayashi, H. and Sheen, J. (1996) Engineered GFP as a vital reporter in plants. *Curr. Biol.* 6: 325-330.

Clough, S.J. and Bent, A.F. (1998) Floral dip: a simplified method for *Agrobacterium*-mediated transformation of *Arabidopsis thaliana*. *Plant J*. 16: 735-743.

Delmas, F., Seveno, M., Northey, J.G., Hernould, M., Lerouge, P., McCourt, P., et al. (2008) The synthesis of the rhamnogalacturonan II component 3-deoxy-D-*manno*-2-octulosonic acid (Kdo) is required for pollen tube growth and elongation. *J. Exp. Bot.* 59: 2639-2647.

Elthon, T.E., Nickels, R.L. and McIntosh, L. (1989) Monoclonal antibodies to the alternative oxidase of higher plant mitochondria. *Plant Physiol.* 89: 1311-1317.

Fleischer, A., Titel, C. and Ehwald, R. (1998) The boron requirement and cell wall properties of growing and stationary suspension-cultured *Chenopodium album* L. cells. *Plant Physiol.* 117: 1401-1410.

Hart, D.A. and Kindel, P.K. (1970) Isolation and partial characterization of apiogalacturonans from the cell wall of *Lemna minor*. *Biochemical J.* 116: 569-579.

Heazlewood, J.L., Tonti-Filippini, J.S., Gout, A.M., Day, D.A., Whelan, J. and Millar, A.H. (2004) Experimental analysis of the Arabidopsis mitochondrial proteome highlights signaling and regulatory components, provides assessment of targeting prediction programs, and indicates plant-specific mitochondrial proteins. *Plant Cell* 16: 241-256.

Iwai, H., Masaoka, N., Ishii, T. and Satoh, S. (2002) A pectin glucuronyltransferase gene is essential for intercellular attachment in the plant meristem. *Proc. Natl Acad. Sci. USA* 99: 16319-16324.

Johnson-Brousseau, S.A. and McCormick, S. (2004) A compendium of methods useful for characterizing *Arabidopsis* pollen mutants and gametophytically-expressed genes. *Plant J.* 39: 761-775.

Kobayashi, M., Nakagawa, H., Asaka, T. and Matoh, T. (1999) Borate-rhamnogalacturonan II bonding reinforced by Ca^{2+} retains pectic polysaccharides in higher-plant cell walls. *Plant Physiol.* 119: 199-204.

Kobayashi, M., Ohno, K. and Matoh, T. (1997) Boron nutrition of cultured tobacco BY-2 cells .II. Characterization of the boron-polysaccharide complex. *Plant Cell Physiol.* 38: 676-683.

Koshiba, T., Kobayashi, M. and Matoh, T. (2009) Boron nutrition of tobacco BY-2 cells. V. oxidative damage is the major cause of cell death induced by boron deprivation. *Plant Cell Physiol.* 50: 26-36.

Koshiba, T., Kobayashi, M., Ishihara, A. and Matoh, T. (2010) Boron nutrition of cultured tobacco BY-2 cells. VI. Calcium is involved in early responses to boron deprivation. *Plant Cell Physiol.* 51: 323-327.

Li, C., Guan, Z., Liu, D. and Raetz, C.R.H. (2011) Pathway for lipid A biosynthesis in *Arabidopsis thaliana* resembling that of *Escherichia coli*. *Proc Natl Acad. Sci. USA* 108: 11387-11392.

Mohnen , D. (2008) Pectin structure and biosynthesis. *Curr. Opin. Plant Biol.* 11: 266–277.

Matoh, T., Ishigaki, K., Mizutani, M., Matsunaga, W. and Takabe, K. (1992) Boron Nutrition of Cultured Tobacco BY-2 Cells. I. Requirement for and intracellular-localization of boron and selection of cells that tolerate low-levels of boron. *Plant Cell Physiol.* 33: 1135-1141.

Matoh, T., Kawaguchi, S. and Kobayashi, M. (1996) Ubiquity of a borate-rhamnogalacturonan II complex in the cell walls of higher plants. *Plant Cell Physiol.* 37: 636-640.

Matoh, T., Takasaki, M., Kobayashi, M. and Takabe, K. (2000) Boron nutrition of cultured tobacco BY-2 cells. III. Characterization of the boron-rhamnogalacturonan II complex in cells acclimated to low levels of boron. *Plant Cell Physiol.* 41: 363-366.

Matsuura, K., Miyagawa, I., Kobayashi, M., Ohta, D. and Matoh, T. (2003) *Arabidopsis* 3-deoxy-D-*manno*-oct-2-ulosonate-8-phosphate synthase: cDNA cloning and expression analyses. *J. Exp. Bot.* 54: 1785-1787.

Misaki, R., Kajiura, H., Fujii, K., Fujiyama, K. and Seki, T. (2009) Cloning and characterization of cytidine monophosphate-3-deoxy-D-*manno*-octulosonate synthetase from *Arabidopsis thaliana*. *J. Biosci. Bioeng*. 108: 527-529.

Nagata, T., Okada, K., Takebe, I. and Matsui, C. (1981) Delivery of tobacco mosaic virus RNA into plant protoplasts mediated by reverse-phase evaporation vesicles (liposomes). *Mol. Gen. Genet.* 184: 161-165.

Obayashi, T., Hayashi, S., Saeki, M., Ohta, H. and Kinoshita, K. (2009) ATTED-II provides coexpressed gene networks for Arabidopsis. *Nucleic Acids Res.* 37: D987-D991.

O'Neill, M.A., Eberhard, S., Albersheim, P. and Darvill, A.G. (2001) Requirement of borate cross-linking of cell wall rhamnogalacturonan II for *Arabidopsis* growth. *Science* 294: 846-849.

Preuss, D., Rhee, S.Y. and Davis, R.W. (1994) Tetrad analysis possible in Arabidopsis with mutation of the QUARTET (QRT) genes. *Science* 264: 1458-1460.

Raetz, C.R.H. (1990) Biochemistry of endotoxins. *Annu. Rev. Biochem.* 59: 129–170.

Royo, J., Gomez, E. and Hueros, G. (2000) A maize homologue of the bacterial CMP-3-deoxy-D-*manno*-2-octulosonate (KDO) synthetases. Similar pathways operate in plants and bacteria for the activation of KDO prior to its incorporation into outer cellular envelopes. *J. Biol. Chem.* 275: 24993-24999.

Ryden, P., Sugimoto-Shirasu, K., Smith, A.C., Findlay, K., Reiter, W.D. and McCann, M.C. (2003) Tensile properties of Arabidopsis cell walls depend on both a xyloglucan cross-linked microfibrillar network and rhamnogalacturonan II-borate complexes. *Plant Physiol.* 132: 1033-1040.

Séveno, M., Séveno-Carpentier, E., Voxeur A., Menu-Bouaouiche, L., Rihouey, C., Delmas, F. et al. (2010) Characterization of a putative 3-deoxy-D-*manno*-2-octulosonic acid (Kdo) transferase gene from *Arabidopsis thaliana*. *Glycobiology* 20: 617-628.

Stevenson, T., Darvill, A.G. and Albersheim, P. (1988) 3-Deoxy-D-*lyxo*-2-heptulosaric acid, a component of the plant cell-wall polysaccharide rhamnogalacturonan-II. *Carbohydr. Res.* 179: 269-288.

Takashima, S., Seino, J., Nakano, T., Fujiyama, K., Tsujimoto, M., Ishida, N. et al. (2009) Analysis of CMP-sialic acid transporter-like proteins in plants. *Phytochemistry* 70: 1973-1981.

Toyooka, K., Goto, Y., Asatsuma, S., Koizumi, M., Mitsui, T. and Matsuoka, K. (2009). A mobile secretory vesicle cluster involved in mass transport from the Golgi to plant cell exterior. *Plant Cell* 21: 1212-1229.

Wimmer, M.A., Lochnit, G., Bassil, E., Muhling, K.H. and Goldbach, H.E. (2009) Membrane-associated, boron-interacting proteins isolated by boronate affinity chromatography. *Plant Cell Physiol.* 50: 1292-1304.

Winter, D., Vinegar, B., Nahal, H., Ammar, R., Wilson, G.V. and Provart, N.J. (2007) An ‘‘Electronic Fluorescent Pictograph’’ browser for exploring and analyzing large-scale biological data sets. *PLoS ONE* 2: e718.

Yuasa, K., Toyooka, K., Fukuda, H. and Matsuoka, K. (2005) Membrane-anchored prolyl hydroxylase with an export signal from the endoplasmic reticulum. *Plant J.* 41: 81-94.

Tables

Table 1 Segregation of selfed progenies of +/*cks* plants

Genotype	Line		
	SALK_008109	SALK_021302	SALK_052743
+/+	28	43	50
+/*cks*	25	55	40
cks/*cks*	0	0	0

Table 2 Analysis of genetic transmission of *cks* genotype by reciprocal test crosses

Parent		Genotype	
		+/+	+/*cks*
Male	Female		
+/+	+/*cks*	17	21
+/*cks*	+/+	50	0

Figure legends

Figure 1

Multiple alignment of CKS-like sequences from plants and bacteria. Sequences from Arabidopsis (*A. thaliana*; NP_175708), maize (*Zea mays*, NP_001105657), rice (*Oryza sativa*, NP_001056314), *Chlamydia trachomatis* (YP_001654510), and *E. coli* (NP_415438) were aligned with ClustalW (http://align.genome.jp/). Arrow in Arabidopsis sequence indicates region expressed as bacterial recombinant protein. Identical and similar residues are shaded in black and gray, respectively.

Figure 2

Characterization of recombinant AtCKS protein. (a) SDS-PAGE of proteins from *E. coli* carrying expression construct with (lane +) or without (lane –) addition of IPTG. Arrowhead indicates expressed recombinant AtCKS protein. (b) Time course of CMP-KDO production measured using bacterial lysate with or without inducing expression of recombinant protein (+IPTG or –IPTG, respectively). (c) pH dependence of activity of partially purified recombinant AtCKS protein. Activity was measured using CTP as the nucleotide donor and expressed as a relative value (value at pH 9.5 =100%). (d) Preference of nucleotide donor of partially purified recombinant AtCKS protein. Assays were carried out at pH 9.5.

Figure 3

Subcellular localization of AtCKS protein. (a) AtCKS fused to GFP at its C-terminus (AtCKS:GFP; upper panels) or GFP alone (lower panels) was expressed in tobacco BY-2 cells under the control of the cauliflower mosaic virus 35S RNA promoter. Cells were fed with MitoTracker dye and observed under a confocal laser scanning microscope. Fluorescence signal from GFP (the first column) and MitoTracker (the second column) were converted into green and magenta, respectively, and merged (the third column). The fourth column represents the

corresponding bright-field images. Bar = 20 μm. (b) AtCKS:GFP was transiently expressed in tobacco BY-2 cells transformed with prolyl hydroxylase fused to mRFP (PH:mRFP), a Golgi marker. Fluorescence signal from GFP (the first column) and mRFP (the second column) were converted into green and magenta, respectively, and merged (the third column). The fourth column represents the corresponding bright-field images. Upper panels: lower magnification, lower panels: higher magnification. Bar = 20 μm. (c) Immunolocalization of AtCKS protein. Ultrathin sections of Arabidopsis root tip were stained with anti-AtCKS antibody and observed under electron microscope. Mt; mitochondria. Bar = 200 nm. (d) Submitochondrial localization of AtCKS protein. The protease thermolysin (TL) was added to a mitochondria-enriched fraction in the presence or absence of Triton X-100 (TX100) to rupture the mitochondrial membranes. Proteins were separated by SDS-PAGE, transferred to a membrane, and probed with anti-CKS antisera or monoclonal anti-mitochondrial alternative oxidase (AOX) antibody.

Figure 4

Identification and characterization of *AtCKS* T-DNA insertion mutants. (a) Schematic representation of *AtCKS* gene (*At1g53000*) and T-DNA insertion sites in the allele. Boxes represent exons and solid lines represent introns. Gray boxes represent protein-coding sequence, arrowheads indicate annealing site of primers. (b) Genotyping of selfed progenies from a SALK_052743 heterozygous (+/*cks*) mutant plant. Genomic DNA extracted from each individual was used as the template for PCR with three primers, 1L, 1R, and LBa1. Wild-type genome shows a band of ca. 1 kb with 1L and 1R, whereas the T-DNA-inserted genome shows a band of ca. 0.6 kb with LBa1 and 1R. Individuals yielding a single 1-kb band were judged as wild-type (w), whereas those gave both 1-kb and 0.6-kb bands were judged as heterozygotes (ht). No homozygous mutant with a single 0.6-kb band was detected. (c) RT-PCR analysis of *AtCKS* transcript abundance in +/*cks* heterozygote. Total RNA was extracted from young leaves

of either wild-type or SALK_052743 heterozygous plants, reverse-transcribed, and PCR-amplified. *Actin* was included in the analysis to calibrate cDNA concentrations.

Figure 5

Characterization of pollen from wild-type and *cks* heterozygous plants. (a) and (b), Mature pollen tetrads from +/*cks*; *qrt1*/*qrt1* plant (SALK_052743) stained with Alexander reagent (a) or 4',6-diamidino-2-phenylindole (DAPI) (b). Bar=50 nm. (c) In vitro-germinated pollen grains from +/+; *qrt1*/*qrt1* (left panel) or +/*cks*; *qrt1*/*qrt1* (right panel) plants. Red arrowheads indicate pollen tetrads with three pollen tubes. White arrowheads indicate short, fat, or irregularly shaped pollen tubes. Bar=100 nm. (d) Frequency distribution of length of pollen tubes produced from in vitro-germinated pollen grains. Shown is the representative result from three independent experiments.

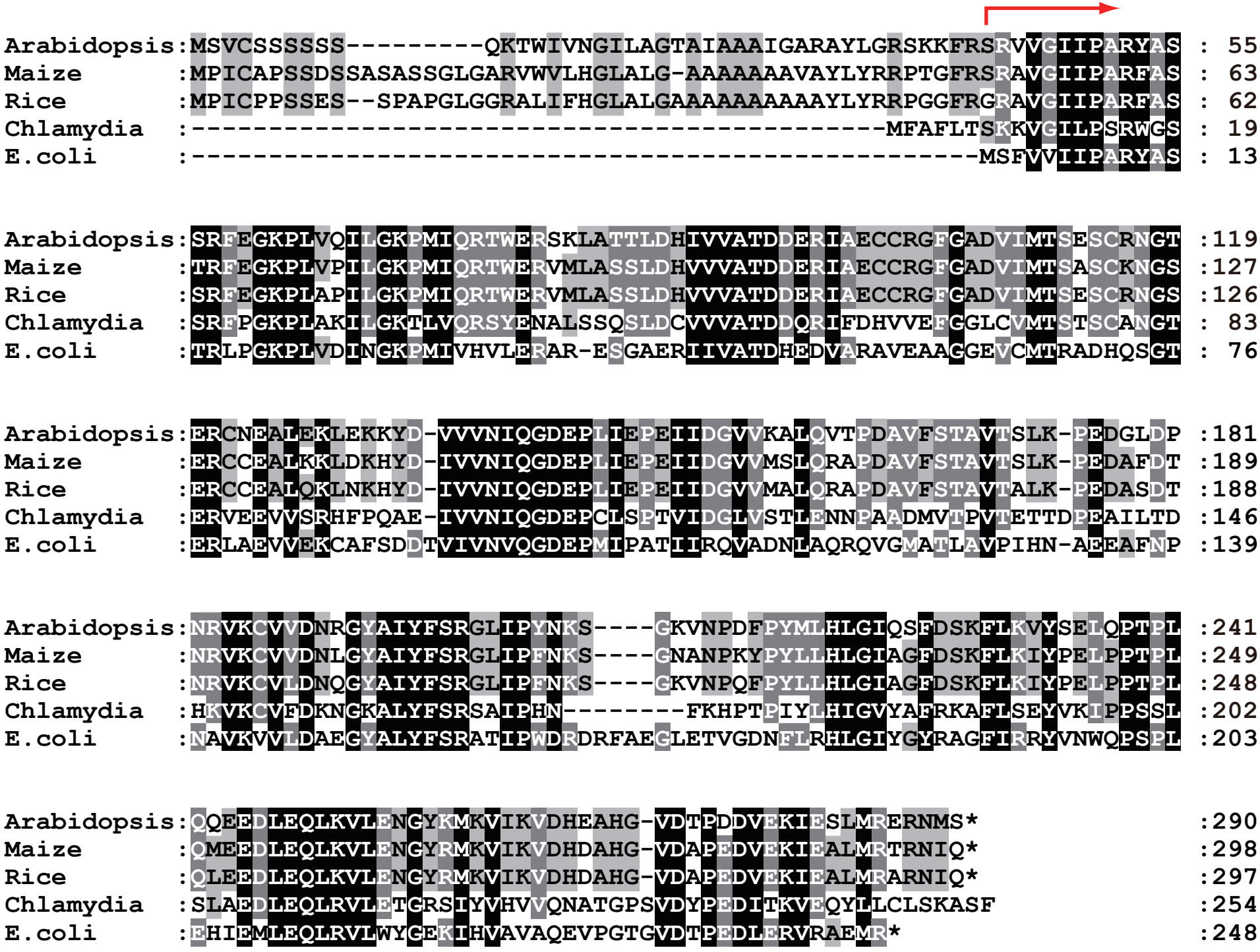
Arabidopsis:MSVCSSSSSS---------QKTWIVNGILAGTAIAAAIGARAYLGRSKKFRSRVVGIIPARYAS : 55
Maize :MPICAPSSDSSASASSGLGARVWVLHGLALG-AAAAAAAVAYLYRRPTGFRSRAVGIIPARFAS : 63
Rice :MPICPPSSES--SPAPGLGGRALIFHGLALGAAAAAAAAAAYLYRRPGGFRGRAVGIIPARFAS : 62
Chlamydia :----------MFAFLTSKKVGILPSRWGS : 19
E.coli :----------MSFVVIIPARYAS : 13
Arabidopsis:SRFEGKPLVQILGKPMIQRTWERSKLATTLDHIVVATDDERIAECCRGFGADVIMTSESCRNGT :119
Maize :TRFEGKPLVPILGKPMIQRTWERVMLASSLDHVVVATDDERIAECCRGFGADVIMTSASCKNGS :127
Rice :SRFEGKPLAPILGKPMIQRTWERVMLASSLDHVVVATDDERIAECCRGFGADVIMTSESCRNGS :126
Chlamydia :SRFPGKPLAKILGKTLVQRSYENALSSQSLDCVVVATDDQRIFDHVVEFGGLCVMTSTSCANGT : 83
E.coli :TRLPGKPLVDINGKPMIVHVLERAR-ESGAERIIVATDHEDVARAVEAAGGEVCMTRADHQSGT : 76
Arabidopsis:ERCNEALEKLEKKYD-VVVNIQGDEPLIEPEIIDGVVKALQVTPDAVFSTAVTSLK-PEDGLDP :181
Maize :ERCCEALKKLDKHYD-IVVNIQGDEPLIEPEIIDGVVMSLQRAPDAVFSTAVTSLK-PEDAFDT :189
Rice :ERCCEALQKLNKHYD-IVVNIQGDEPLIEPEIIDGVVMALQRAPDAVFSTAVTALK-PEDASDT :188
Chlamydia :ERVEEVVSRHFPQAE-IVVNIQGDEPCLSPTVIDGLVSTLENNPAADMVTPVTETTDPEAILTD :146
E.coli :ERLAEVVEKCAFSDDTVIVNVQGDEPMIPATIIRQVADNLAQRQVGMATLAVPIHN-AEEAFNP :139
Arabidopsis:NRVKCVVDNRGYAIYFSRGLIPYNKS----GKVNPDFPYMLHLGIQSFDSKFLKVYSELQPTPL :241
Maize :NRVKCVVDNLGYAIYFSRGLIPFNKS----GNANPKYPYLLHLGIAGFDSKFLKIYPELPPTPL :249
Rice :NRVKCVLDNQGYAIYFSRGLIPFNKS----GKVNPQFPYLLHLGIAGFDSKFLKIYPELPPTPL :248
Chlamydia :HKVKCVFDKNGKALYFSRSAIPHN--------FKHPTPIYLHIGVYAFRKAFLSEYVKIPPSSL :202
E.coli :NAVKVVLDAEGYALYFSRATIPWDRDRFAEGLETVGDNFLRHLGIYGYRAGFIRRYVNWQPSPL :203
Arabidopsis:QQEEDLEQLKVLENGYKMKVIKVDHEAHG-VDTPDDVEKIESLMRERNMS* :290
Maize :QMEEDLEQLKVLENGYRMKVIKVDHDAHG-VDAPEDVEKIEALMRTRNIQ* :298
Rice :QLEEDLEQLKVLENGYRMKVIKVDHDAHG-VDAPEDVEKIEALMRARNIQ* :297
Chlamydia :SLAEDLEQLRVLETGRSIYVHVVQNATGPSVDYPEDITKVEQYLLCLSKASF :254
E.coli :EHIEMLEQLRVLWYGEKIHVAVAQEVPGTGVDTPEDLERVRAEMR* :248

Figure 1

Figure 2

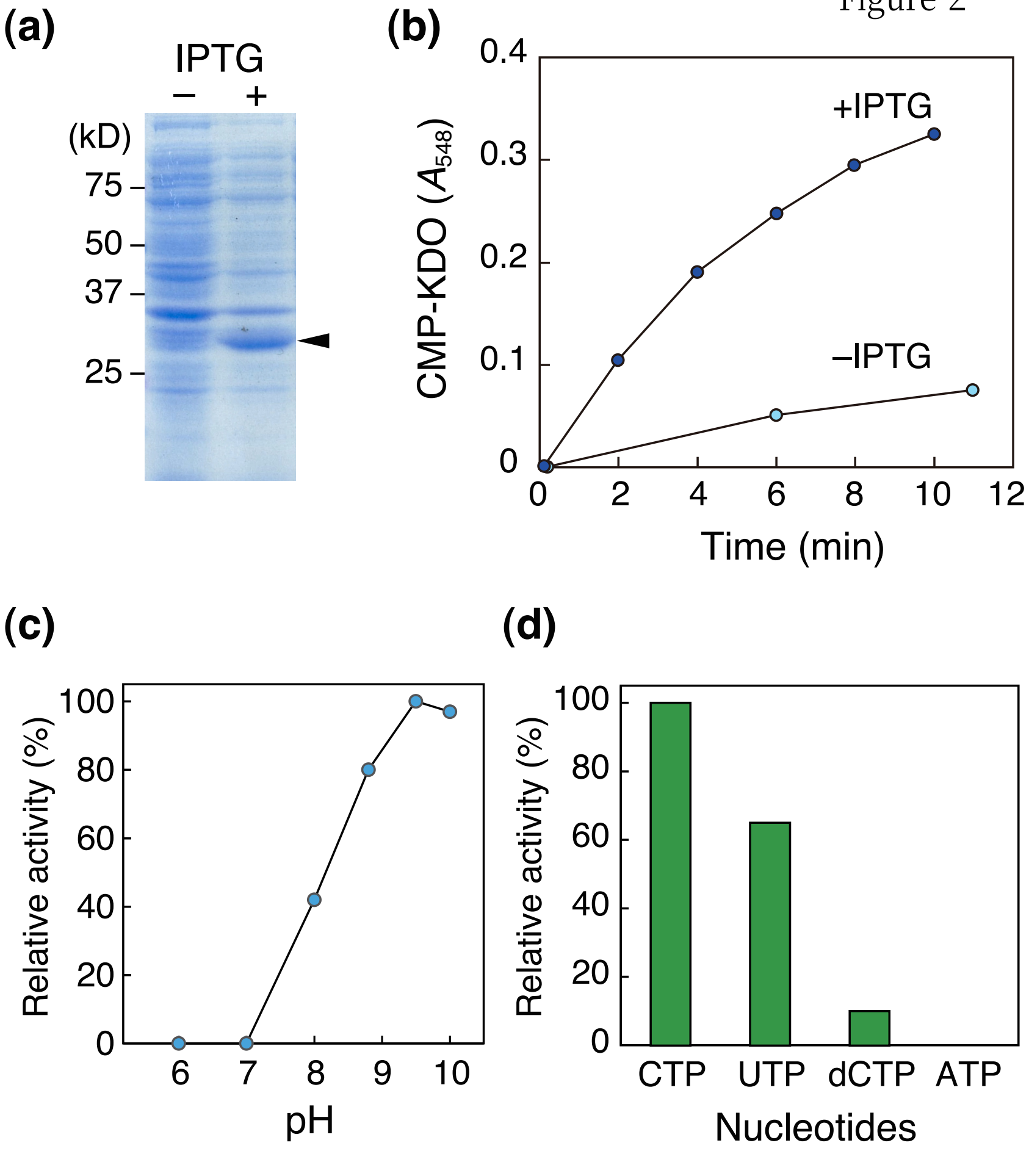
(a)
IPTG
–
+
(kD)
75
50
37
25
(b)
CMP-KDO (A_{548})
0.4
0.3
0.2
0.1
0
+IPTG
–IPTG
0
2
4
6
8
10
12
Time (min)
(c)
Relative activity (%)
100
80
60
40
20
0
6
7
8
9
10
pH
(d)
Relative activity (%)
100
80
60
40
20
0
CTP
UTP
dCTP
ATP
Nucleotides

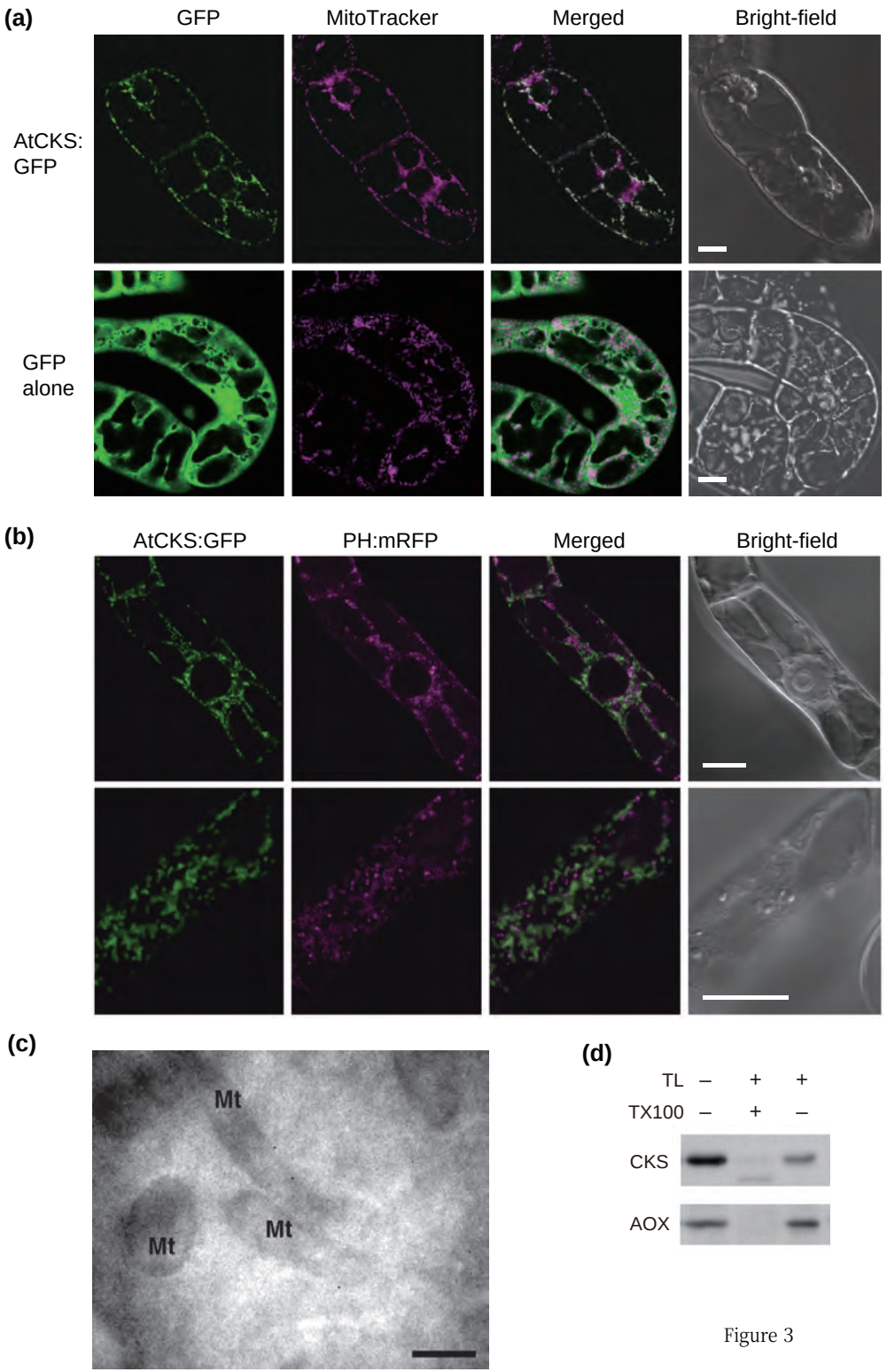
(a)
GFP
MitoTracker
Merged
Bright-field
AtCKS: GFP
GFP alone
(b)
AtCKS:GFP
PH:mRFP
Merged
Bright-field
(c)
Mt
Mt
Mt
(d)
TL – + +
TX100 – + –
CKS
AOX

Figure 3

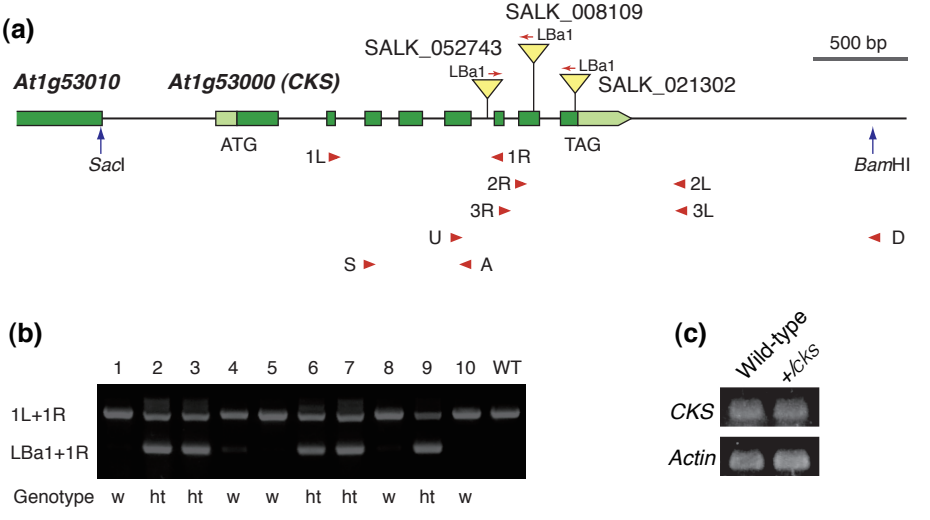
(a)
SALK_008109
LBa1
SALK_052743
LBa1
LBa1
SALK_021302
500 bp
At1g53010
At1g53000 (CKS)
SacI
ATG
1L
1R
TAG
BamHI
2R
2L
3R
3L
U
D
S
A
(b)
1 2 3 4 5 6 7 8 9 10 WT
1L+1R
LBa1+1R
Genotype w ht ht w w ht ht w ht w
(c)
Wild-type
+cks
CKS
Actin

Figure 4

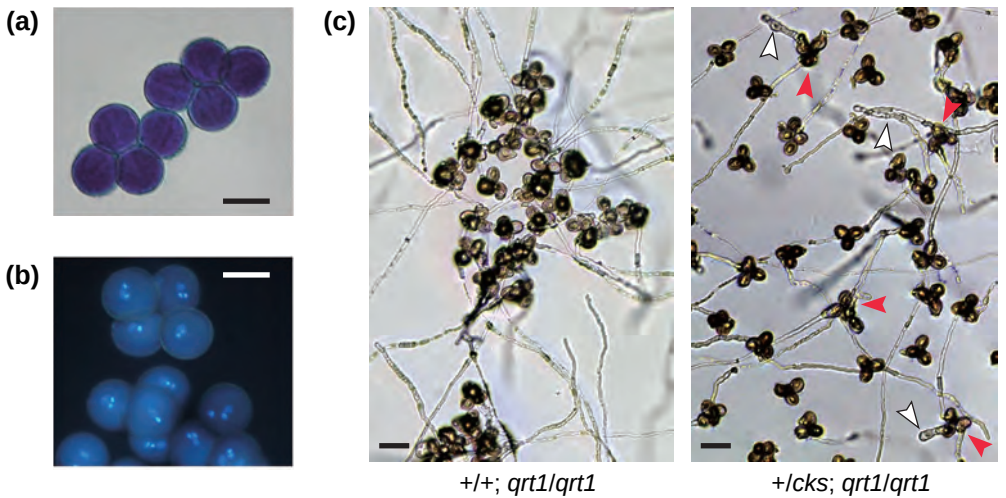
(a)
(b)
(c)
+/+; qrt1/qrt1
+/cks; qrt1/qrt1

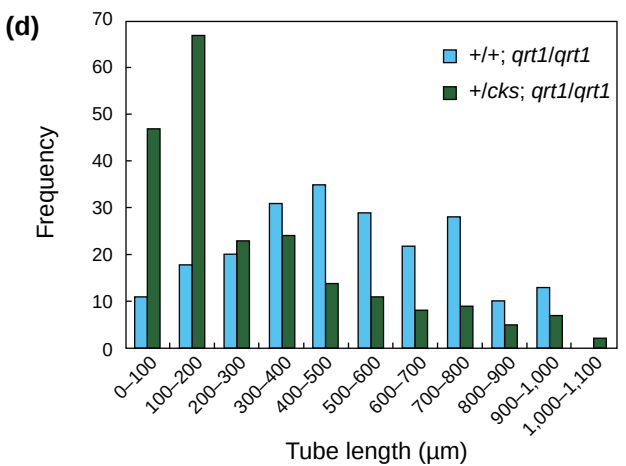
(d)
Frequency
70
60
50
40
30
20
10
0
+/+; qrt1/qrt1
+/cks; qrt1/qrt1
0–100
100–200
200–300
300–400
400–500
500–600
600–700
700–800
800–900
900–1,000
1,000–1,100
Tube length (μm)

Figure 5

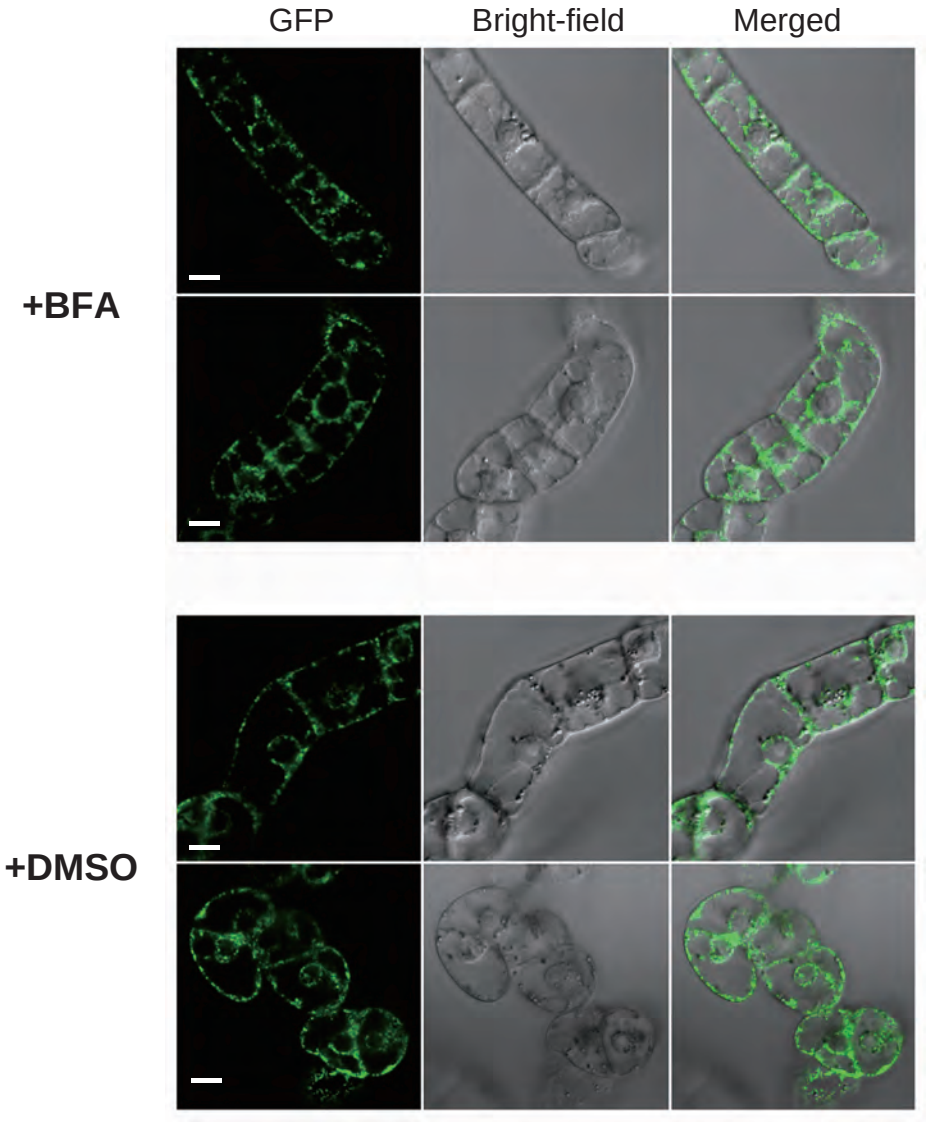

Supplementary Figure S1.
Effect of brefeldin A (BFA) on the distribution of fluorescence signal from AtCKS:GFP. Three-day-old tobacco BY-2 cells expressing AtCKS:GFP were fed with BFA dissolved in dimethylsulfoxide (DMSO) (upper two rows) or equivalent concentration of DMSO as a control (lower two rows). BFA was added at a final concentration of 5 µg ml^{-1}. Fluorescence signal from AtCKS:GFP (left), corresponding bright-field image (middle), and merged image (right) are shown for two representative optical sections from each treatment. Bar = 20 µm.